Published in final edited form as:
Gastroenterology. 2012 August ; 143(2): 469–480. doi:10.1053/j.gastro.2012.04.011.

Induced Mist1 Expression Promotes Remodeling of Mouse Pancreatic Acinar Cells

Daniel Direnzo[*], **David A. Hess**[*], **Barbara Damsz**[*], **Judy E. Hallett**[*], **Brett Marshall**[*], **Chirayu Goswami**[‡], **Yunlong Liu**[‡], **Tye Deering**[§], **Raymond J. Macdonald**[§], and **Stephen F. Konieczny**[*]

[*]Department of Biological Sciences and the Purdue Center for Cancer Research, Purdue University, West Lafayette, Indiana

[‡]Laboratory for Computational Genomics, Indiana University School of Medicine, Indianapolis, Indiana

[§]Department of Molecular Biology, University of Texas Southwestern Medical Center, Dallas, Texas

Abstract

BACKGROUND & AIMS—Early embryogenesis involves cell fate decisions that define the body axes and establish pools of progenitor cells. Development does not stop once lineages are specified; cells continue to undergo specific maturation events, and changes in gene expression patterns lead to their unique physiological functions. Secretory pancreatic acinar cells mature postnatally to synthesize large amounts of protein, polarize, and communicate with other cells. The transcription factor MIST1 is expressed by only secretory cells and regulates maturation events. MIST1-deficient acinar cells in mice do not establish apical-basal polarity, properly position zymogen granules, or communicate with adjacent cells, disrupting pancreatic function. We investigated whether MIST1 directly induces and maintains the mature phenotype of acinar cells.

METHODS—We analyzed the effects of Cre-mediated expression of *Mist1* in adult *Mist1*–deficient ($Mist1^{KO}$) mice. Pancreatic tissues were collected and analyzed by light and electron microscopy, immunohistochemistry, real-time polymerase chain reaction analysis, and chromatin immunoprecipitation. Primary acini were isolated from mice and analyzed in amylase secretion assays.

RESULTS—Induced expression of *Mist1* in adult $Mist1^{KO}$ mice restored wild-type gene expression patterns in acinar cells. The acinar cells changed phenotypes, establishing apical-basal polarity, increasing the size of zymogen granules, reorganizing the cytoskeletal network, communicating intercellularly (by synthesizing gap junctions), and undergoing exocytosis.

Reprint requests. Address requests for reprints to: Stephen F. Konieczny, PhD, Department of Biological Sciences and the Purdue Center for Cancer Research, Purdue University, Hansen Life Sciences Research Building, 201 South University Street, West Lafayette, Indiana 47907-2064. sfk@purdue.edu; fax: (765) 496-2536.

Supplementary Material

Note: To access the supplementary material accompanying this article, visit the online version of *Gastroenterology* at www.gastrojournal.org, and at http://dx.doi.org/10.1053/j.gastro.2012.04.011.

Conflicts of interest

The authors disclose no conflicts.

CONCLUSIONS—The exocrine pancreas of adult mice can be remodeled by re-expression of the transcription factor MIST1. MIST1 regulates acinar cell maturation and might be used to repair damaged pancreata in patients with pancreatic disorders.

Keywords

DIMM; Exocrine Pancreas Disease; Secretion; Transcription

Although vertebrate embryogenesis is responsible for the initial establishment of individual cell fates, most cells require additional maturation events to ensure their appropriate specialization in the adult organism. These events often include creation of intracellular polarity, setting up cell– cell communication, and expanding (qualitative and quantitative) gene expression patterns so that cells are able to perform their unique functions. Despite significant progress in defining transcriptional networks that control early cell fate decisions, little is known about how key transcription factors regulate maturation events. This is a particularly important area of investigation because genetic alterations that disrupt the specialization properties of differentiated cells often lead to disease states. Thus, defining the transcriptional circuits that maintain the adult cell phenotype is critical for devising intervention strategies for different diseases.

The exocrine pancreas serves as an excellent model to study cell maturation events. A hallmark of the adult exocrine organ is formation of well-organized acini units consisting of individual acinar cells that show an apical-basal cellular polarity, clustering of zymogen granules, and extensive intercellular signaling networks. The initial specification of the cells begins early in mouse pancreas development (~embryonic day 12.5), but final maturation, including accumulation of abundant rough endoplasmic reticulum, maximum expression of digestive enzyme transcripts, apically localized zymogen granules, and the ability to regulate exocytosis events, occurs during late embryonic and postnatal development.[1–3] A key protein involved in this maturation process is MIST1 (also known as BHLHA15), a basic helix-loop-helix transcription factor whose expression in the pancreas is restricted to acinar cells.[4,5] Embryonic *Mist1* null (*Mist1*^{KO}) acinar cells fail to establish an apical-basal organization, fail to position zymogen granules, and fail to generate intercellular communication.[4–6] The block in the final differentiation steps leads to a damaged exocrine pancreas that shows defective exocytosis properties,[4,7,8] altered cell proliferation,[9] and a lack of appropriate cell– cell junctions,[6] making the exocrine organ highly susceptible to pancreatic diseases including pancreatitis and pancreatic cancer.[6,7,10]

The *Mist1* gene is unique in that it is expressed exclusively in secretory lineages including salivary gland acinar cells, zymogenic cells of the stomach, lactating mammary epithelial cells, Paneth cells of the intestine, and in antibody- secreting plasma cells.[4,5,11–13] DIMM, the *Drosophila* ortholog of MIST1, is expressed similarly in secretory peptidergic neurons that produce neuropeptides.[14–16] The MIST1/DIMM expression patterns suggest that these proteins have a central role in controlling specific secretory properties associated with each of these differentiated cell types. Indeed, studies by Tian et al[17] have shown that MIST1 controls expression of the small guanosine triphosphatase genes *Rab26* and *Rab3d*, both of which are critical to forming appropriate zymogen granules in stomach zymogenic cells. Similarly, DIMM activates several genes involved in regulated secretion of neuropeptides.[14] In all cases, activation or repression of MIST1/DIMM target genes occurs via binding to specific E-box regulatory elements.[14,17–19]

Studying maturation events in adult pancreatic cells has been hampered by a lack of a tractable genetic system in which changes in cell organization can be followed within the context of the intact organ. To address this question, we generated a novel system in which

expression of a Mist1 transgene was induced in disorganized *Mist1*^{KO} acinar cells within the context of the adult mouse pancreas. Our studies show the remarkable ability of the *Mist1* transcriptional network to restore wild-type gene expression patterns to *Mist1*^{KO} acinar cells. The altered gene expression produced dramatic changes in cellular phenotypes, including generation of apical-basal polarity, increased zymogen granule size, reorganization of the actin cytoskeletal network, and restoration of intercellular communication. In addition, regulated exocytosis function was fully restored upon MIST1 induction. Each of these changes occurred in adult acinar cells in the absence of cell regeneration. These results show that the injured adult exocrine pancreas can be remodeled via expression of a single transcription factor, offering new research paradigms in repairing damaged organs.

Materials and Methods

Mouse Strains and Genotyping

Mist1$^{CreER/+}$ and *Mist1*$^{CreER/CreER}$ mice have been described previously.[10,20] The LSL-Mist1^{myc} transgene was generated by replacing the *LacZ* gene with a myc-tagged *Mist1* coding sequence in the pCAG-CAT-LacZ plasmid that contains a Lox-STOP-Lox cassette.[21] Pronuclear injections and generation of *LSL-Mist1*^{myc} mice were performed by the Purdue University Transgenic Mouse Core Facility. Genotyping and recombination primer sets are listed in the Supplementary Materials and Methods section. Induction of Cre-ER^{T2} activity was accomplished by single administration of tamoxifen (200 μL of 20 mg/mL) via oral gavage to adult mice (8–9 wk). All experiments were performed with mice on a C57BL/6 background, and all animal studies were conducted in compliance with the National Institutes of Health and the Purdue University IACUC guidelines.

Histology and Immunohistochemistry

Mouse pancreata were fixed in 10% neutral buffered formalin, embedded in paraffin, sectioned, and stained using conventional histologic techniques. Tissue sections were deparaffinized and retrieved using the 2100-Retriever (Pick-Cell Laboratories, Amsterdam, The Netherlands) and antigen unmasking solution (Vector Laboratories, Burlingame, CA). Blocking was performed by incubating sections with 3% H_2O_2 for 10 minutes and using the M.O.M. blocking kit (Vector Laboratories). Primary antibodies were applied for 1 hour at room temperature or 4°C overnight with biotinylated secondary antibodies added for 10 minutes at room temperature. Visualization was accomplished via diaminobenzidine peroxidase staining (Vector Laboratories) or tertiary, avidin-conjugated Alexa Fluor 594 (Invitrogen, Camarillo, CA). Primary antibodies and conditions are provided in the Supplementary Materials and Methods section.

Electron Microscopy

Pancreata were fragmented into 1-mm cubes and fixed in 3% paraformaldehyde/0.5% glutaraldehyde in phosphate-buffered saline, gradually dehydrated, and embedded in Epon resin (Electron Microscopy Sciences, Hatfield, PA). Electron micrographs were obtained from ultra-thin sections using a Philips CM-100 transmission electron microscope (Philips, Andover, MA).

RNA Expression Analysis

Pancreatic RNA was isolated using the RNeasy system (Qiagen, Valencia, CA). RNA processing, hybridization, and initial analysis of the Affymetrix Mouse Gene 1.0 ST expression arrays (Affymetrix, Santa Clara, CA) was performed by the Indiana University Center for Medical Genomics according to the manufacturer's protocols. The complete set

of .CEL files is available at the National Center for Biotechnology Information Gene Expression Omnibus (GEO accession number GSE34232). For real-time polymerase chain reaction (PCR) analysis, RNA was converted to complementary DNA using the iScript complementary DNA synthesis kit (Bio-Rad, Hercules, CA) and amplified with FastStart Universal SYBR Green (Roche Applied Science, Indianapolis, IN) using an ABI 7300 Real-Time PCR System (Applied Biosystems, Foster City, CA). Real-time PCR primers are listed in the Supplementary Materials and Methods section.

Chromatin Immunoprecipitation

Mouse pancreata were disrupted using a dounce homogenizer and fixed in 1% formaldehyde for 10 minutes. Fixation was quenched in 125 mmol/L glycine for 5 minutes, and nuclei were disrupted with 10 mL lysis buffer (10 mmol/L Tris-HCl, pH 7.5, 10 mmol/L NaCl, 3 mmol/L $MgCl_2$, 0.5% octylphenoxypoly-ethoxyethanol, and 1 mmol/L phenylmethylsulfonyl fluoride). Samples then were sonicated 5 times and precleared with Protein A sepharose beads (GE Healthcare, Latham, NY). Incubation with 2 μg anti-MIST1 or control IgG was performed overnight at 4°C with rocking. Bound protein/DNA complexes were resuspended in TE buffer supplemented with 195 mmol/L NaCl. Cross-linking was reversed by incubation at 65°C overnight and digested with proteinase K at 56°C for 4 hours. DNA was purified using a Qiaquick PCR purification kit (Qiagen) and used for real-time PCR.

Isolated Acini

Primary acini were isolated from *wild-type* (*WT*), *Mist1*^{KO}, and *Mist1*^{KO}/*LSL-Mist1*^{myc} mice as described previously.[10] Single-cell injections of 6-carboxyfluorescein (Invitrogen) were imaged 3 minutes after injection. Amylase secretion assays were performed using published protocols.[22] Briefly, whole pancreata were isolated, washed in Hank's Balanced Salt Solution, and injected with 0.1 mg/mL collagenase P (Roche Applied Science) in serum-free media supplemented with bovine serum albumin. Pancreata then were rocked at 37°C for 40 minutes in fresh collagenase P solution, sheared via passage through narrow-orifice pipettes, and filtered through 150-μm nylon cloth. Isolated acini were washed, given a 30-minute rest period at 37°C, and then stimulated with 30 μmol/L cholecystokinin. Supernatants and cell pellets were collected for quantification of percentage amylase release via the Infinity Amylase Detection Kit (ThermoFisher Scientific, Waltham, MA).

Results

Establishing an Inducible *Mist1* Mouse Model

Mouse pancreatic acinar cells are specified during early pancreatic development but final maturation of the cells occurs postnatally and is dependent on an intact MIST1 transcriptional network (Figure 1*A*).[1–3,5,6] Given the importance of maturation events to a normal exocrine pancreas, we asked if activation of a single transcription factor in damaged adult acinar cells could re-establish maturation properties and cell function. To this end, we developed an inducible transgenic mouse line that expressed a myc-tagged MIST1 protein upon Cre-mediated recombination of an upstream Lox-STOP-Lox cassette (*LSL-Mist1*^{myc}) (Figure 1*B*). Crossing *LSL-Mist1*^{myc} mice to *Mist1*$^{CreER/+}$ mice[10,20] generated *Mist1*$^{CreER/CreER}$/*LSL-Mist1*^{myc} offspring that lacked the endogenous *Mist1* allele (*Mist1*^{KO}/*LSL-Mist1*^{myc}). Upon exposure to tamoxifen (TM), the transcriptional LSL stop cassette was excised and expression of Mist1^{myc} was driven by the constitutive CAG promoter exclusively in acinar cells (Figure 1*C* and *D*).[21] Mist1^{myc}-expressing cells were observed as early as 6 hours after TM, with peak response (~90% acinar cells) achieved by 24 hours (Figure 1*E*). Importantly, no overt phenotype was observed in the acinar, ductal, or

islet cell compartments of *Mist1*$^{CreER/+}$ (*Mist1*^{HET})/*LSL-Mist1*^{myc} mice that maintained constitutive Mist1^{myc} expression for more than 3 months (Supplementary Figure 1*A* and *B*).

Genome-Wide Expression Changes Upon *Mist1*^{myc} Induction

The *Mist1*^{KO} phenotype suggested that *Mist1* operates postnatally to maintain acinar cell organization and function in the adult organ. To test this hypothesis, we asked if induced MIST1^{myc} could shift acinar gene expression profiles and reverse the disorganized exocrine pancreas of adult *Mist1*^{KO} organs. We chose 36 hours after TM as a time point when approximately 90% of *Mist1*^{KO} acinar cells expressed the *LSL-Mist1*^{myc} transgene and reasoned that this sampling would allow us to identify early changes in adult gene expression patterns owing to induced MIST1^{myc}.

WT, Mist1^{KO}, and *Mist1*^{KO}*/LSL-Mist1*^{myc} littermates (4 per group) were given a single dose of TM, after which pancreatic RNA was harvested 36 hours after TM, converted to complementary DNA, and hybridized to Affymetrix Gene 1.0 ST expression arrays. Principal component analysis revealed a clear separation in gene expression profiles between *Mist1*^{KO} and *WT* pancreata (Figure 2*A*). Interestingly, within 36 hours of inducing *LSL-Mist1*^{myc}, the gene expression signature of *Mist1*^{KO}*/LSL-Mist1*^{myc} pancreata was remodeled with an overall shift in gene expression profiles approaching *WT* signatures (Figure 2*A* and *B*). Analysis of the array data revealed a cohort of 949 genes ($P < .05$; fold-change, >1.5) that were expressed differentially between WT and *Mist1*^{KO} pancreata (Figure 2*B* and *C*). Of these, 353 (37%) were classified as fully rescued in *Mist1*^{KO}*/LSL-Mist1*^{myc} samples, with 186 genes up-regulated and 166 genes down-regulated within this short time frame. A gene was considered fully rescued if its relative array expression value was within 25% of *WT* levels. For example, MIST1^{myc}-activated genes that had ≥75% of *WT* levels and MIST1^{myc}-repressed genes that were ≤125% of *WT* levels were considered fully rescued. Similarly, 145 genes (15%) had a partial rescue profile, reaching 50%–74% (activated genes) or 126%–150% (repressed genes) of *WT* expression levels by 36 hours (Figure 2*B* and *C*). Another 98 genes had significant qualitative differences but only modest quantitative changes toward *WT* levels (<50% for activated genes and >150% for repressed genes). Interestingly, 354 genes (37%) that showed significant differences in expression between *WT* and *Mist1*^{KO} pancreata remained unchanged in the *Mist1*^{KO}*/LSL-Mist1*^{myc} samples, suggesting that these were target genes that responded slowly to MIST1^{myc} or were genes with altered expression patterns in adult *Mist1*^{KO} pancreata but were not direct MIST1 gene targets (Figure 2*B* and *C*).

Specific *Mist1* Gene Targets

The gene array analyses identified a cassette of acinar genes that rapidly responded to induced MIST1^{myc} expression in the adult organ. To understand the functional significance of gene expression changes, we focused on 20 genes for the following reasons: (1) they were significantly up-regulated or down-regulated upon MIST1^{myc} induction, (2) they were identified previously as potential MIST1 targets (*connexin32* [*Cx32*], *Atp2c2*, and *Rab3d*),[6,17,23] (3) they contained potential MIST1 binding sites, and (4) their gene products likely were critical to normal acinar cell function (Supplementary Figure 2). Pancreatic RNA was isolated from adult *Mist1*^{KO}*/LSL-Mist1*^{myc} mice 1–21 days after TM, and the transcript levels of individual genes were determined by reverse-transcription quantitative PCR and compared with *WT* and *Mist1*^{KO} pancreata RNA expression levels. As shown in Figure 3*A* and *B*, a number of genes (*Rab3d, Htra2, Uba5, Rab27a, Abcb6, Slc35d1, Nox4, Gstm4, Nfe2l2*, and *Rnd2*) showed rapid transcript changes (up and down) that approached *WT* levels by 24 hours after TM and that were maintained at near *WT* levels over the 3-week time course. In contrast, other genes (*Cx32, Atp2c2, Wdyhv1, Copz2, Foxp2, Aldh1a1, Ptgr1, Cldn10, Ppap2b*, and *Smarca1*) showed a gradual change in transcript levels that

nonetheless achieved *WT* levels over the 21-day period. Regardless of the differences in rates of expression, the MIST1^{myc}-induced up-regulated and down-regulated changes were specific to this gene set because the expression profiles for a number of other genes were not significantly different between *WT* and *Mist1^{KO}* samples and remained unresponsive to MIST1^{myc} expression (Figure 3C). Likewise, induction of MIST1^{myc} in *Mist1$^{CreER/+}$* mice had no effect on the expression of putative MIST1 target genes, including *Cx32, Atp2c2*, and *Rnd2* (Supplementary Figure 1*C*). These results confirm that increased *Mist1* expression per se does not lead to misregulation of the acinar cell transcriptome. Instead, it is the induction of MIST1^{myc} in a damaged *Mist1^{KO}* background that generates specific gene expression changes.

The robust responses of the 20 candidate genes to MIST1^{myc} suggested that they are direct MIST1 targets. To test this hypothesis, chromatin immunoprecipitation (ChIP) assays were performed with anti-MIST1 antibody on *WT* pancreata to identify MIST1 binding sites. Initial PCR primer pairs were chosen based on 2 criteria: a focus on the 5' promoter and first intronic regions of each gene and on ChIP-seq results, which tentatively identified MIST1 binding sites within the mouse genome. As predicted, most genes showed MIST1-specific ChIP enrichment with the exception of *Nox4*, which showed no enrichment with several different primer sets (Figure 4). Sequence analysis revealed a significant concentration of GC or TA E-box target sites situated at or near the ChIP amplicon regions for most of the putative target genes (Supplementary Figure 3), suggesting that MIST1 activates or represses gene expression through direct binding to E-box regulatory elements located within the promoter and first intronic regions.[18] Several exceptions were found that lacked proximal regulatory sites including the *Slc35d1, Atp2c2, Cldn10*, and *Ppap2b* genes, in which the predicted (by ChIP-seq) and confirmed MIST1 binding sites were considerably distal (+11 kb → +54 kb) to the transcription start sites. The combined gene expression and ChIP analyses support the idea that induced Mist1^{myc} affects gene expression by binding to promoters, distant enhancers, or introns of its target genes to promote or repress gene transcription.

Adult Remodeling of the Exocrine Pancreas Upon *Mist1^{myc}* Expression

Although identification of individual MIST1 target genes provides a roadmap to understanding the molecular mechanisms by which MIST1 regulates gene expression, the focus of this study was to investigate if induced MIST1^{myc} could reverse exocrine defects in an adult intact organ. To examine this possibility, we administered TM to *WT, Mist1^{KO}*, and *Mist1^{KO}/LSL-Mist1^{myc}* mice, and then harvested pancreata at 1, 3, 7, and 21 days after treatment. Multiple tissue samples from each time point were examined for known defects associated with the *Mist1^{KO}* exocrine pancreas, including alterations in cellular organization, zymogen granule dynamics, and ductal lumen size.

As previously reported,[5] *Mist1^{KO}* acinar cells lacked an apical-basal polarity in which nuclei and rough endoplasmic reticulum normally accumulate at the basal aspect and zymogen granules cluster at the apical pole (Figure 5*A* and *B*). However, expression of the *LSL-Mist1^{myc}* transgene re-established the characteristic cellular polarity observed in *WT* pancreata. Within 24 hours, nuclei began to accumulate basally, with near-complete cellular reorganization by 7 days after TM (Figure 5*A* and *B*). As part of this reorganization, aberrant zymogen granule localization also was rescued, with enhanced zymogen granule clustering evident by 1 day after TM (Figure 5*B* and *C*; Supplementary Figure 4*A*). Similarly, the smaller-sized zymogen granules found in *Mist1^{KO}* acinar cells rapidly achieved *WT* diameters within 4 days after TM (Figure 5*C*; Supplementary Figure 4*B*). Interestingly, acinar reorganization was entirely owing to changes in the current adult cell population. There was no evidence of altered acinar cell regeneration during the 3-week time course (unpublished results).

Another key characteristic of pancreatic acini were the apical, tight junction– dependent lumens where secreted zymogens enter the ductal system. Typical *WT* lumens were focal and small whereas *Mist1*^{KO} acini lumens were highly dilated, with reduced secretion content (Figure 5*D and E*). Induction of MIST1^{myc} in *Mist1*^{KO}/*LSL-Mist1*^{myc} mice rapidly led to closure of the lumen openings (Figure 5*D* and *E*). Changes in lumen sizes also were accompanied by alterations in the actin cytoskeleton and in the overall size of MIST1^{myc}-expressing acinar cells. Although *Mist1*^{KO} acinar cells were small and lacked a significant cortical and terminal actin web,[5] induction of MIST1^{myc} re-established the actin cytoskeleton (Figure 6*A*). Likewise, MIST1^{myc} expression led to increases in the size of *Mist1*^{KO} acinar cells but had no affect on islet cell size within the same tissue (Figure 6*B*). The basal level of autophagy that previously was reported for *Mist1*^{KO} acinar cells[5] also was completely eliminated within 3 days of MIST1^{myc} induction (Figure 6*C* and *D*). Together, these studies place MIST1 within a critical transcriptional network that controls the organization of the acinar cell cytoskeleton to maintain proper apical-basal polarity and zymogen granule dynamics. Similarly, the constant state of physiological stress in the absence of MIST1 is rescued by induced expression of *LSL-Mist1*^{myc} in adult cells.

Mist1 Regulates Acinar Cell Communication and Secretion

MIST1 is essential for efficient cell–cell communication owing, at least in part, to up-regulation of the gap-junction protein Cx32.[6,8] Indeed, *Mist1*^{KO} acinar cells were completely devoid of Cx32-containing gap junctions (Figure 7*A*). To determine if induced MIST1^{myc} could re-establish gap junction complexes, *Mist1*^{KO}/*LSL-Mist1*^{myc} pancreata were examined for restoration of Cx32 gap junctions over a 3-week post-TM period. As predicted from the *Cx32* transcript analysis (Figure 3*A*), Cx32 gap junctions assembled on adult *Mist1*^{KO}/*LSL-Mist1*^{myc} acinar cells by 3 days after TM (Figure 7*A* and *B*). In addition, the newly synthesized gap junctions were fully functional. Single-cell injections of 6-carboxyfluorescein into isolated acini confirmed that the transport of 6-carboxyfluorescein into neighboring cells was restored within 3 days of MIST1^{myc} expression (Figure 7*C*), showing that adult acinar cell intercellular communication can be remodeled by ectopic MIST1 protein.

Finally, to examine if induced MIST1^{myc} could rescue functional exocytosis in *Mist1*^{KO} acinar cells, we performed amylase secretion assays on adult *WT, Mist1*^{KO}, and *Mist1*^{KO}/*LSL-Mist1*^{myc} mice 7 days after TM. As previously reported,[8] *Mist1*^{KO} acini were completely unresponsive to cholecystokinin induction of regulated exocytosis (Figure 7*D*). However, *Mist1*^{KO} mice expressing MIST1^{myc} showed restored amylase secretion that reached *WT* acinar cell efficiencies 7 days after TM (Figure 7*D*). Together, these studies show that the defects observed in *Mist1*^{KO} granule secretion can be recovered robustly and quickly by expression of exogenous MIST1^{myc} in quiescent, adult pancreatic acinar cells within the context of the intact organ.

Discussion

Embryonic cell fate decisions define the body axes and establish progenitor cell pools that direct organogenesis. Much has been learned about the transcriptional networks that are instrumental in permitting cell lineages to develop where loss of key transcription factors can have devastating consequences to this initial body plan. Although the importance of cell fate choices is obvious, development does not cease after cells commit to a specific lineage. Instead, most cells undergo a further type–specific maturation in which changes in the cellular transcriptome are needed to ensure proper gene products are available for cells to perform their unique physiological functions.[24]

Understanding the molecular pathways instrumental in cell maturation has been hampered by a lack of inducible systems in which the course of specialization can be followed in the intact organ. In this study, we asked if induced MIST1 expression could remodel the adult exocrine pancreas because *Mist1*^{KO}-associated defects leave the organ susceptible to bouts of pancreatitis and pancreatic cancer.[7,10] We found that within 36 hours of MIST1 induction, the expression of 352 genes was qualitatively and quantitatively rescued, with 186 up-regulated and 166 down-regulated. Detailed analysis of a cohort of genes confirmed the presence of MIST1-bound regulatory elements that contained CATATG and CAGCTG E-boxes, the preferred binding sites of the vertebrate MIST1 and *Drosophila* DIMM proteins.[14,17,23,25] The ability of MIST1 to activate and repress different target genes was expected because previous studies have shown that MIST1/DIMM serve as transcriptional activators or repressors depending on the gene context.[6,9,17–19,23,25]

Investigation of 20 target genes revealed that their functions were involved intimately in the specialization of acinar cells, namely generating correct cellular polarity and establishing a proper secretory pathway. The expression profiles of genes encoding a tight junction protein (*Cldn10*) involved in cell polarity[26] and a Rho guanosine triphosphatase (*Rnd2*) that regulates actin cytoskeletal dynamics[27] were restored to *WT* levels upon MIST1^{myc} induction. Similarly, a group of genes (*Rab3d, Rab27a, Atp2c2, Gjb1*, and *Copz2*) known to be critical for exocytosis were mis-expressed in *Mist1*^{KO} acinar cells and rescued by MIST1^{myc}. *Gjb1*, which encodes Cx32, is critical to gap junction formation, allowing cells to use an intercellular Ca^{2+} signaling cascade for efficient secretion.[6] *Mist1*^{KO} acinar cells failed to express *Gjb1*, but this defect readily was reversed by MIST1^{myc} expression, which restored Cx32 gap junctions and intercellular communication. The genes encoding RAB3D and RAB27A, small guanosine triphosphatases that are known to be important in vesicle trafficking,[17,28] and COPZ2, a subunit of the coatomer protein complex involved in vesicle formation,[29] also were up-regulated upon MIST1^{myc} expression, leading to proper zymogen granule trafficking and increased vesicle size. These results were in agreement with Tian et al,[17] who showed that forced expression of MIST1 in gastric cell lines led to up-regulation of *Rab3d* and increased vesicle formation. Similarly, the mis-expression of DIMM in *Drosophila* peptidergic neurons induces genes encoding dense-core vesicle proteins.[25] MIST1^{myc} also rapidly induced the expression of *Atp2c2*, the gene encoding the acinar secretory pathway Ca^{2+}-adenosine triphosphatase[23] and rescued the Ca^{2+}-dependent exocytosis defects associated with loss of *Mist1*.

We also identified additional genes (*Htra2, Uba5, Abcb6, Nox4, Gstm4, Nfe2I2*, and *Aldh1a1*) that regulate cellular stress pathways. *Htra2* encodes a serine protease that plays a protective role against cellular stress.[30] Similarly, *Nfe2I2*, encoding a basic leucine zipper transcription factor, activates antioxidant and cellular detoxification programs by targeting specific downstream modulators.[31] Another MIST1 target gene was *Uba5*, encoding an E1-like, ubiquitin-activating enzyme that activates the post-translational modifier protein ubiquitin fold modifier 1.[32] Ubiquitin fold modifier 1 is expressed to high levels in acinar cells and protects pancreatic cells from ER stress–induced apoptosis.[33] In agreement with these altered gene expression profiles, *Mist1*^{KO} acinar cells have shown deficient ER-stress pathway responses[7] and increased levels of autophagy[5] that completely were ameliorated by expression of MIST1^{myc}. Of the identified stress-related genes that came out of our rescue screens, only one (*Nox4*) was found to not bind MIST1 protein. Interestingly, *Nox4* transcription is regulated by *Nfe2I2*,[34] which itself is a MIST1 gene target. Future studies will focus on mapping the entire regulatory network by which MIST1 controls aspects of acinar cell function.

MIST1 is a unique transcription factor in that it functions primarily to ensure the correct qualitative and quantitative expression levels of specific secretory cell genes to establish

proper, regulated, high-capacity exocytosis. Recently, Mills and Taghert[35] proposed that MIST1/DIMM be classified as "scaling factors" that are tasked with controlling entire subcellular domains associated with a mature cell type. In support of this idea, our studies revealed that MIST1 indeed controls aspects of acinar cell organization that are involved in regulated exocytosis events. The importance of MIST1 to maintaining cellular organization also is apparent in a number of pancreatic diseases in which loss of *Mist1* exacerbates pancreatitis and pancreatic cancer formation.[7,10] Similarly, loss of MIST1 is a prognostic indicator of gastric carcinomas.[36,37] Indeed, alteration of intracellular organization is likely critical to disease formation in many different organ contexts. The ability of *Mist1* to alter the phenotype of an adult acinar cell offers new therapeutic opportunities for treating a number of diseases, including pancreatitis and pancreatic cancer.

Supplementary Material

Refer to Web version on PubMed Central for supplementary material.

Acknowledgments

The authors thank the Purdue Center for Cancer Research Transgenic Mouse Core Facility for generating the transgenic mouse strains used in this study and David Miley for generating tissue sections.

Funding

This work was supported by grants from the National Institutes of Health (DK55489 and CA124586 to S.F.K., and DK61220 to R.J.M.), a grant from Phi Beta Psi Sorority (S.F.K.), and a Clinical and Translational Sciences Institute Predoctoral Fellowship (D.D.).

Abbreviations used in this paper

ChIP	chromatin immunoprecipitation
Cre-ER	Cre recombinase-estrogen receptor
Cx32	connexin32
PCR	polymerase chain reaction
TM	tamoxifen
WT	wild type

References

1. de Assis GF, Cestari TM, Sesso A, et al. Post-natal maturation of acinar cells of the guinea pig pancreas: an ultrastructural morphometric study. Anat Histol Embryol. 2003; 32:36–41. [PubMed: 12733271]
2. Jamieson JD, Gorelick FS, Chang A. Development of secretagogue responsiveness in the pancreas. Scand J Gastroenterol Suppl. 1988; 151:98–103. [PubMed: 2852401]
3. Rovira M, Delaspre F, Massumi M, et al. Murine embryonic stem cell-derived pancreatic acinar cells recapitulate features of early pancreatic differentiation. Gastroenterology. 2008; 135:1301–1310. 1310, e1–e5. [PubMed: 18725222]
4. Johnson CL, Kowalik AS, Rajakumar N, et al. Mist1 is necessary for the establishment of granule organization in serous exocrine cells of the gastrointestinal tract. Mech Dev. 2004; 121:261–272. [PubMed: 15003629]
5. Pin CL, Rukstalis JM, Johnson C, et al. The bHLH transcription factor Mist1 is required to maintain exocrine pancreas cell organization and acinar cell identity. J Cell Biol. 2001; 155:519–530. [PubMed: 11696558]

6. Rukstalis JM, Kowalik A, Zhu L, et al. Exocrine specific expression of Connexin32 is dependent on the basic helix-loop-helix transcription factor Mist1. J Cell Sci. 2003; 116:3315–3325. [PubMed: 12829745]
7. Kowalik AS, Johnson CL, Chadi SA, et al. Mice lacking the transcription factor Mist1 exhibit an altered stress response and increased sensitivity to caerulein-induced pancreatitis. Am J Physiol Gastrointest Liver Physiol. 2007; 292:G1123–G1132. [PubMed: 17170023]
8. Luo X, Shin DM, Wang X, et al. Aberrant localization of intracellular organelles, Ca2+ signaling, and exocytosis in Mist1 null mice. J Biol Chem. 2005; 280:12668–12675. [PubMed: 15665001]
9. Jia D, Sun Y, Konieczny SF. Mist1 regulates pancreatic acinar cell proliferation through p21 CIP1/WAF1. Gastroenterology. 2008; 135:1687–1697. [PubMed: 18762186]
10. Shi G, Zhu L, Sun Y, et al. Loss of the acinar-restricted transcription factor Mist1 accelerates Kras-induced pancreatic intraepithelial neoplasia. Gastroenterology. 2009; 136:1368–1378. [PubMed: 19249398]
11. Ramsey VG, Doherty JM, Chen CC, et al. The maturation of mucussecreting gastric epithelial progenitors into digestive-enzyme secreting zymogenic cells requires Mist1. Development. 2007; 134:211–222. [PubMed: 17164426]
12. Bredemeyer AJ, Geahlen JH, Weis VG, et al. The gastric epithelial progenitor cell niche and differentiation of the zymogenic (chief) cell lineage. Dev Biol. 2009; 325:211–224. [PubMed: 19013146]
13. Capoccia BJ, Lennerz JK, Bredemeyer AJ, et al. Transcription factor MIST1 in terminal differentiation of mouse and human plasma cells. Physiol Genomics. 2011; 43:174–186. [PubMed: 21098683]
14. Park D, Shafer OT, Shepherd SP, et al. The Drosophila basic helix-loop-helix protein DIMMED directly activates PHM, a gene encoding a neuropeptide-amidating enzyme. Mol Cell Biol. 2008; 28:410–421. [PubMed: 17967878]
15. Hamanaka Y, Park D, Yin P, et al. Transcriptional orchestration of the regulated secretory pathway in neurons by the bHLH protein DIMM. Curr Biol. 2010; 20:9–18. [PubMed: 20045330]
16. Park D, Taghert PH. Peptidergic neurosecretory cells in insects: organization and control by the bHLH protein DIMMED. Gen Comp Endocrinol. 2009; 162:2–7. [PubMed: 19135054]
17. Tian X, Jin RU, Bredemeyer AJ, et al. RAB26 and RAB3D are direct transcriptional targets of MIST1 that regulate exocrine granule maturation. Mol Cell Biol. 2010; 30:1269–1284. [PubMed: 20038531]
18. Tran T, Jia D, Sun Y, et al. The bHLH domain of Mistl is sufficient to activate gene transcription. Gene Expr. 2007; 13:241–253. [PubMed: 17605298]
19. Lemercier C, To RQ, Carrasco RA, et al. The basic helix-loop-helix transcription factor Mist1 functions as a transcriptional repressor of myoD. EMBO J. 1998; 17:1412–1422. [PubMed: 9482738]
20. Habbe N, Shi G, Meguid RA, et al. Spontaneous induction of murine pancreatic intraepithelial neoplasia (mPanIN) by acinar cell targeting of oncogenic Kras in adult mice. Proc Natl Acad Sci U S A. 2008; 105:18913–18918. [PubMed: 19028870]
21. Araki K, Araki M, Miyazaki J, et al. Site-specific recombination of a transgene in fertilized eggs by transient expression of Cre recombinase. Proc Natl Acad Sci U S A. 1995; 92:160–164. [PubMed: 7816809]
22. Williams, JA. [Accessed November 13, 2010] Isolation of rodent pancreatic acinar cells and acini by collagenase digestion. The Pancreapedia: Exocrine Knowledge Base. 2010. Available at: http://dx.doi.org/10.3998/panc.2010.18
23. Garside VC, Kowalik AS, Johnson CL, et al. MIST1 regulates the pancreatic acinar cell expression of Atp2c2, the gene encoding secretory pathway calcium ATPase 2. Exp Cell Res. 2010; 316:2859–2870. [PubMed: 20599950]
24. MacDonald RJ, Swift GH, Real FX. Transcriptional control of acinar development and homeostasis. Prog Mol Biol Transl Sci. 2010; 97:1–40. [PubMed: 21074728]
25. Park D, Hadzic T, Yin P, et al. Molecular organization of Drosophila neuroendocrine cells by dimmed. Curr Biol. 2011; 21:1515–1524. [PubMed: 21885285]

26. Inai T, Sengoku A, Guan X, et al. Heterogeneity in expression and subcellular localization of tight junction proteins, claudin-10 and -15, examined by RT-PCR and immunofluorescence microscopy. Arch Histol Cytol. 2005; 68:349–360. [PubMed: 16505581]
27. Pacary E, Heng J, Azzarelli R, et al. Proneural transcription factors regulate different steps of cortical neuron migration through Rnd-mediated inhibition of RhoA signaling. Neuron. 2011; 69:1069–1084. [PubMed: 21435554]
28. Kasai K, Ohara-Imaizumi M, Takahashi N, et al. Rab27a mediates the tight docking of insulin granules onto the plasma membrane during glucose stimulation. J Clin Invest. 2005; 115:388–396. [PubMed: 15690086]
29. Moelleken J, Malsam J, Betts MJ, et al. Differential localization of coatomer complex isoforms within the Golgi apparatus. Proc Natl Acad Sci U S A. 2007; 104:4425–4430. [PubMed: 17360540]
30. Moisoi N, Klupsch K, Fedele V, et al. Mitochondrial dysfunction triggered by loss of HtrA2 results in the activation of a brainspecific transcriptional stress response. Cell Death Differ. 2009; 16:449–464. [PubMed: 19023330]
31. Chanas SA, Jiang Q, McMahon M, et al. Loss of the Nrf2 transcription factor causes a marked reduction in constitutive and inducible expression of the glutathione S-transferase Gsta1, Gsta2, Gstm1, Gstm2, Gstm3 and Gstm4 genes in the livers of male and female mice. Biochem J. 2002; 365:405–416. [PubMed: 11991805]
32. Zheng M, Gu X, Zheng D, et al. UBE1DC1, an ubiquitin-activating enzyme, activates two different ubiquitin-like proteins. J Cell Biochem. 2008; 104:2324–2334. [PubMed: 18442052]
33. Lemaire K, Moura RF, Granvik M, et al. Ubiquitin fold modifier 1 (UFM1) and its target UFBP1 protect pancreatic beta cells from ER stress-induced apoptosis. PLoS One. 2011; 6:e18517. [PubMed: 21494687]
34. Pendyala S, Moitra J, Kalari S, et al. Nrf2 regulates hyperoxiainduced Nox4 expression in human lung endothelium: identification of functional antioxidant response elements on the Nox4 promoter. Free Radic Biol Med. 2011; 50:1749–1759. [PubMed: 21443946]
35. Mills JC, Taghert PH. Scaling factors: transcription factors regulating subcellular domains. Bioessays. 2012:3410–3416.
36. Lennerz JK, Kim SH, Oates EL, et al. The transcription factor MIST1 is a novel human gastric chief cell marker whose expression is lost in metaplasia, dysplasia, and carcinoma. Am J Pathol. 2010; 177:1514–1533. [PubMed: 20709804]
37. Nam KT, Lee HJ, Sousa JF, et al. Mature chief cells are cryptic progenitors for metaplasia in the stomach. Gastroenterology. 2010; 139:2028 e9–2037 e9. [PubMed: 20854822]

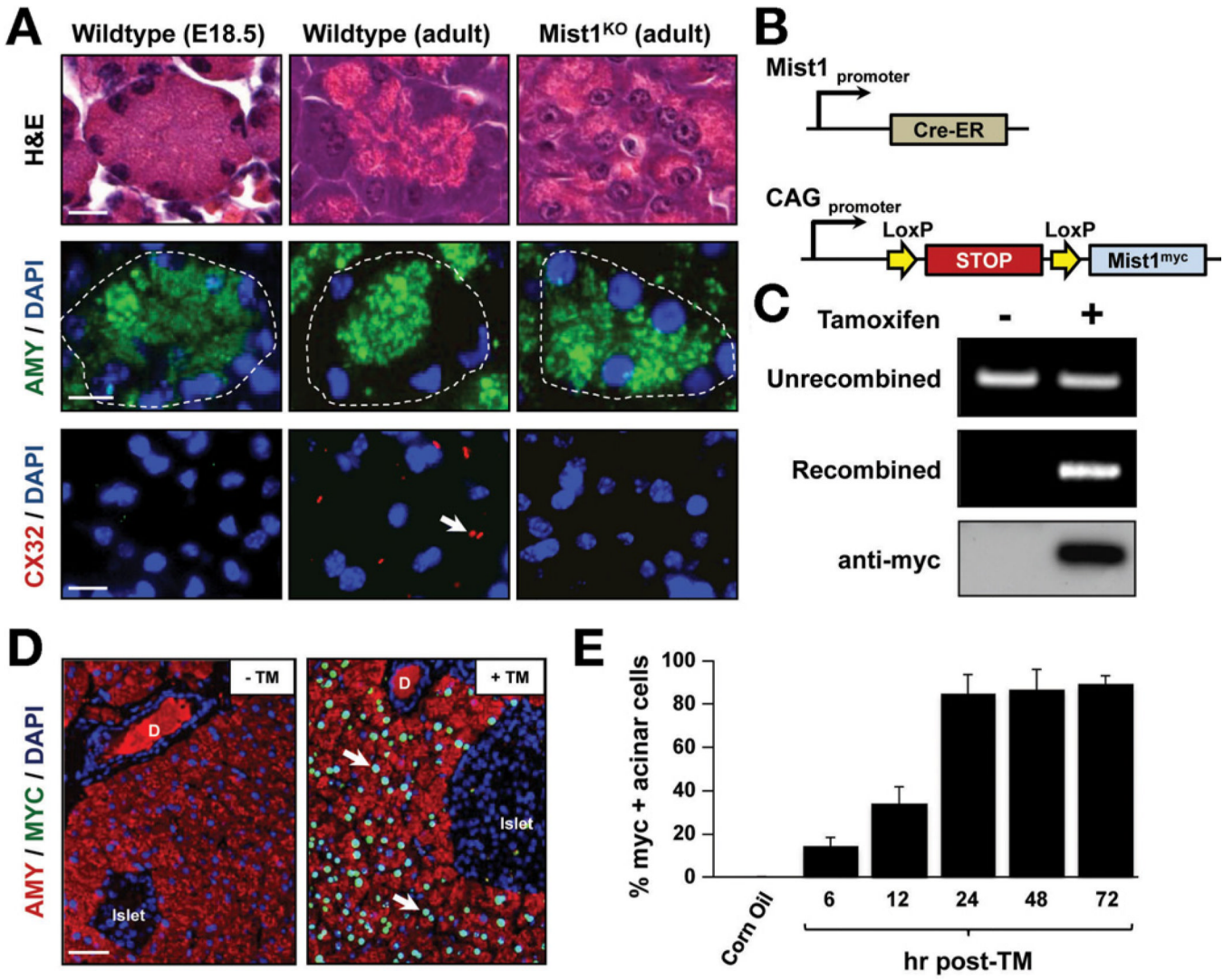

Figure 1.

Characterization of the *LSL-Mist1*^{myc} transgenic line. (*A*) Standard H&E, amylase (AMY), and Cx32 immunofluorescence depicts adult *Mist1*^{KO} acini showing similarities to embryonic cells, in contrast to adult, fully developed *WT* acinar cells. *Arrows*, Cx32 gap junctions. E, embryonic day. (*B*) Schematic of the *Mist1*$^{Cre-ER}$ genomic locus and *LSL-Mist1*^{myc} transgene. (*C*) Genomic PCR and immunoblots reveal the TM-restricted recombination and expression of the *LSL-Mist1*^{myc} transgene. (*D*) Upon TM, only acinar cells express nuclear MIST1^{myc}.protein (*arrows*). D, duct. (*E*) Time-course of MIST1^{myc} expression after TM treatment. *Scale bars*: (*A*) 10 μm; (*D*) 50 μm.

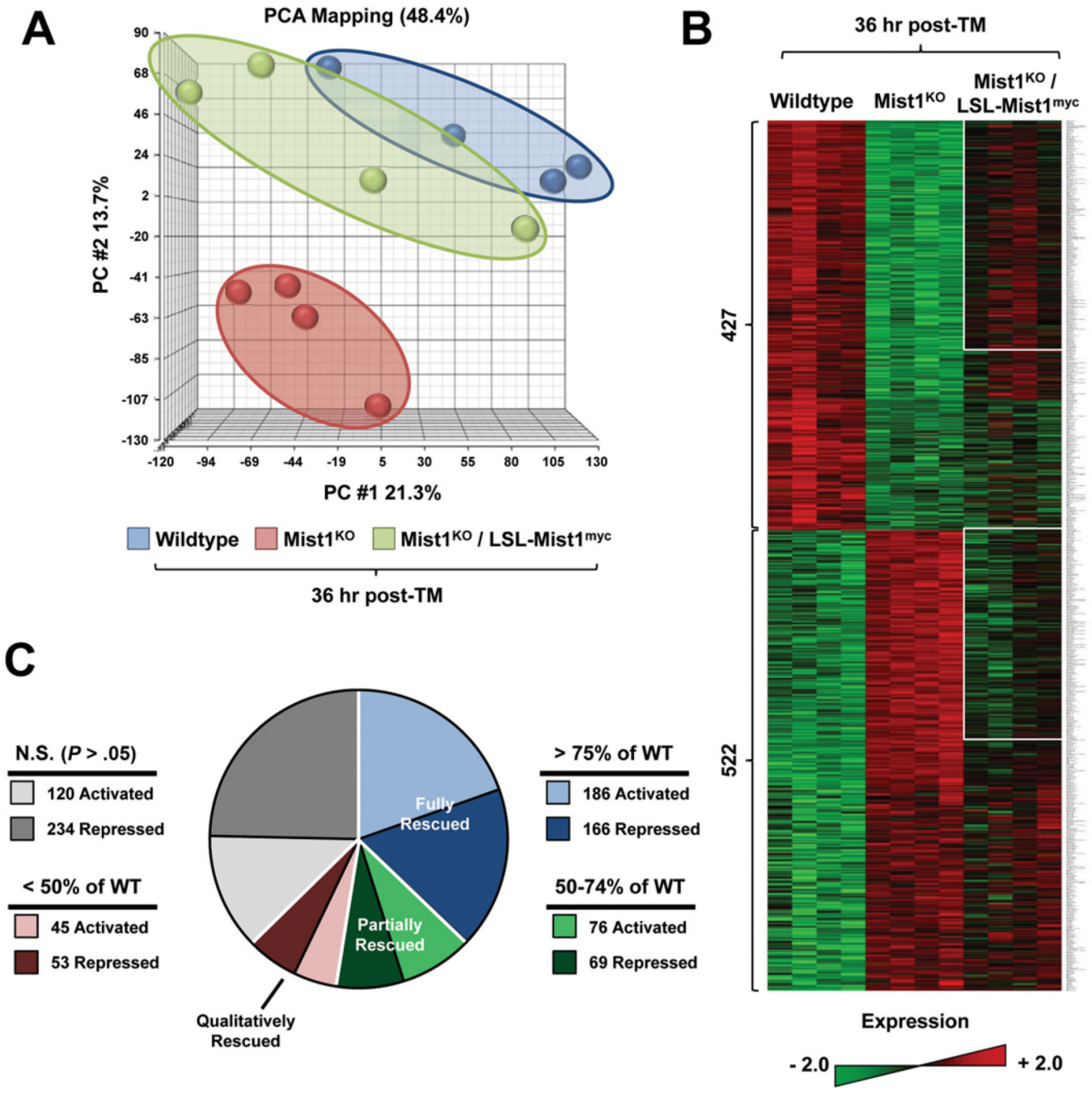

Figure 2.

Expression of *LSL-Mist1*^{myc} for 36 hours induces extensive changes in gene expression. (*A*) Principle component analysis (PCA) of *WT, Mist1*^{KO}, and *Mist1*^{KO}*/LSLMist1*^{myc} mice after TM. Each *small circle* represents an individual animal. See the Supplementary Materials and Methods section for details. (*B*) Representative heat map of 4 individual *WT, Mist1*^{KO}, and *Mist1*^{KO}*/LSL-Mist1*^{myc} pancreas RNA samples. The 949 genes that showed a significant difference in expression ($P < .05$; fold-change, >1.5) between *WT* and *Mist1*^{KO} are indicated. *White boxes* represent fully and partially rescued genes. (*C*) Pie chart illustrating the degree of recovery for the 949 identified genes in *Mist1*^{KO}*/LSL-Mist1*^{myc} mice after TM. See the text for details.

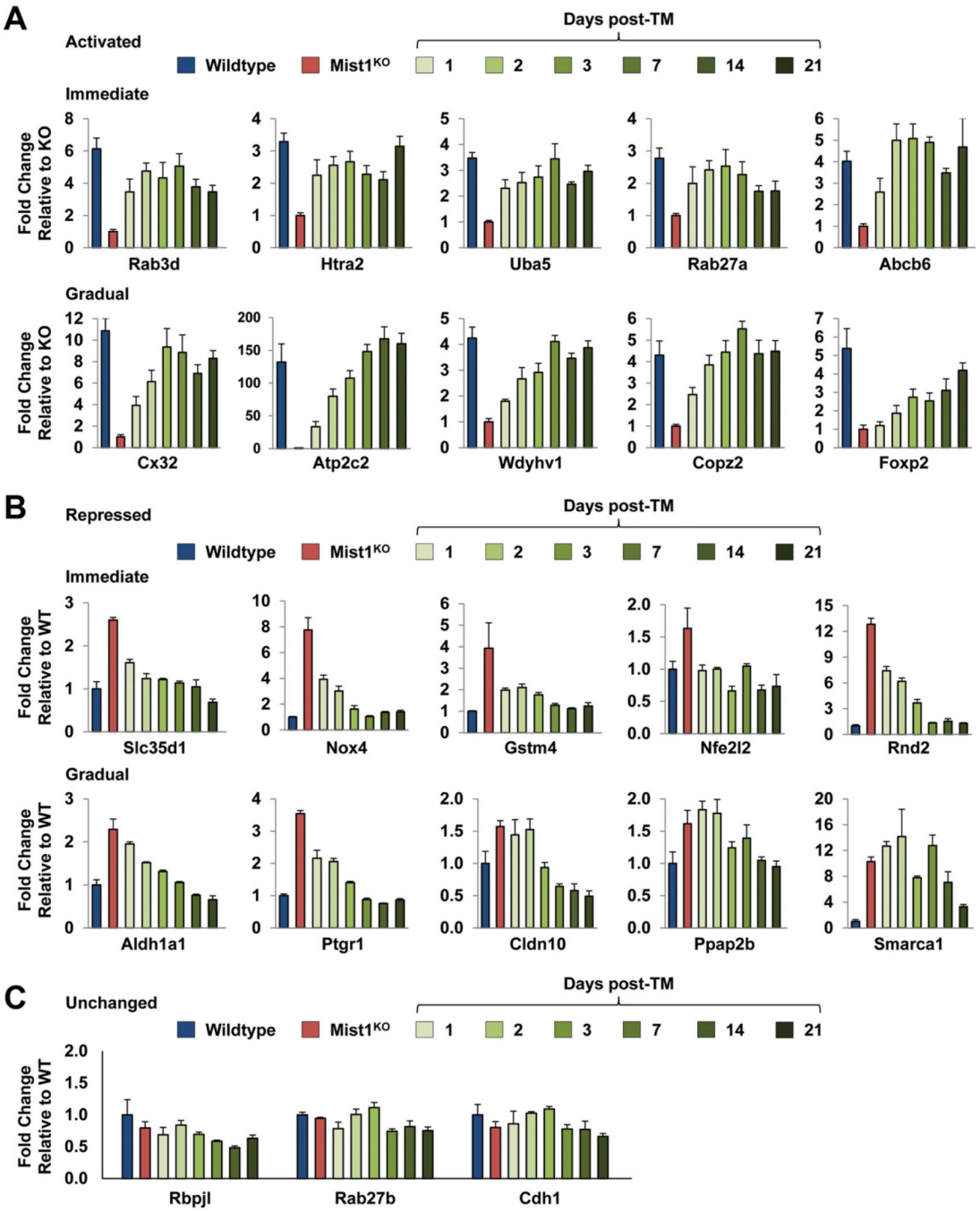

Figure 3.

Long-term expression of *LSL-Mist1*^{myc} further influences gene expression patterns in pancreatic acinar cells. (*A* and *B*) *Mist1*^{KO}*/LSL-Mist1*^{myc} mice (3 mice per time point) were given a single dose of TM and then RNA was harvested at the indicated times. Reverse-transcription quantitative PCR was used to compare the expression profiles of genes from *WT, Mist1*^{KO}, and *Mist1*^{KO}*/LSL-Mist1*^{myc} pancreata. (*C*) Control genes *Rbpjl, Rab27b*, and *Cdh1* show no significant changes in gene expression over this time-course.

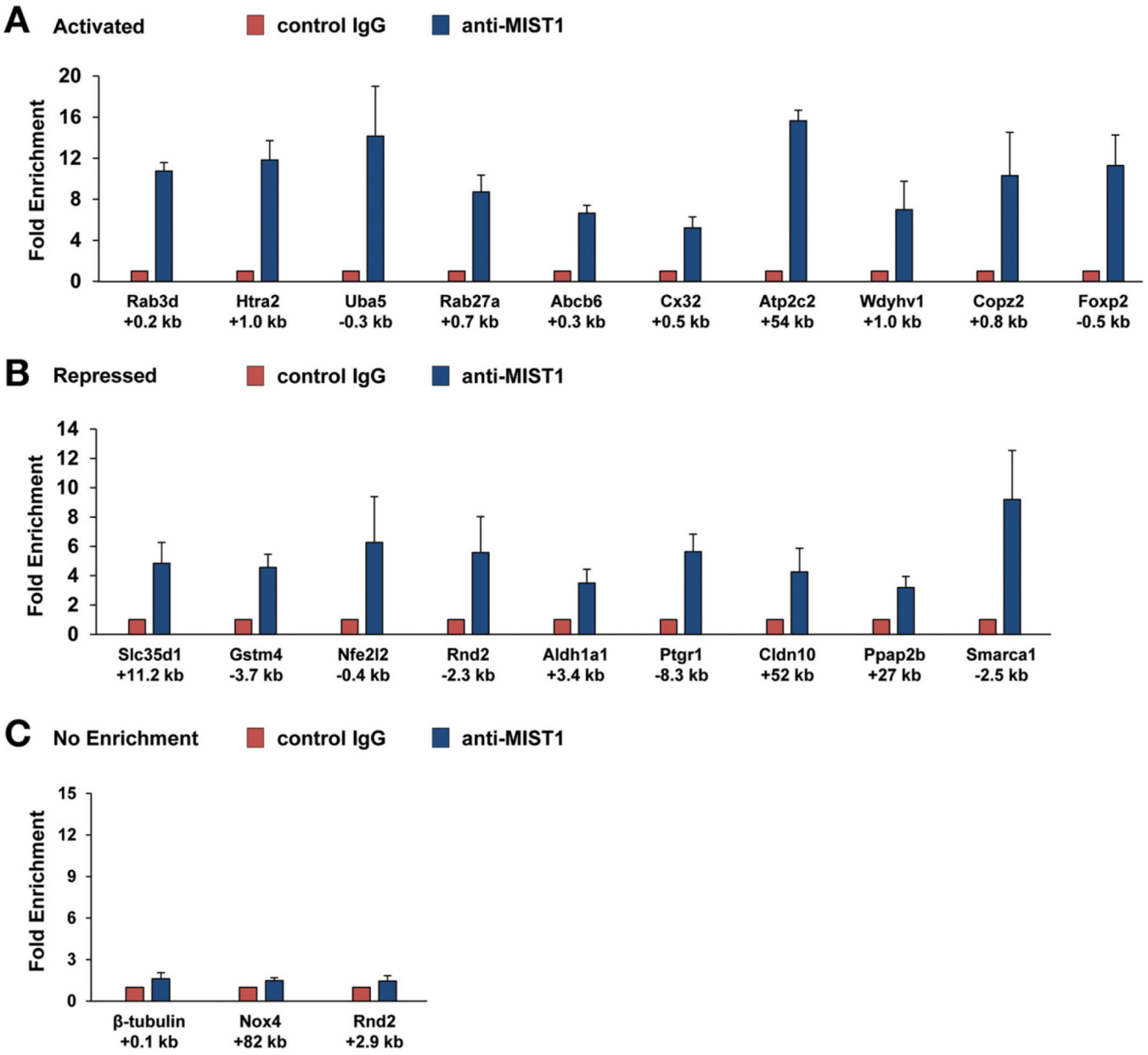

Figure 4.

Chromatin immunoprecipitation assays confirm MIST1 interaction with target genes. (*A* and *B*) Pancreas chromatin from 3 *WT* mice was processed for ChIP assays using anti-IgG (control) or anti-MIST1. In most cases, MIST1 binding was enriched significantly in the anti-Mist1 groups. (*C*) Notably, no enrichment was observed with control genes (β-*tubulin*) or at alternative sites within target genes (eg, *Rnd2* +2.9 kb). In addition, *Nox4* showed no MIST1 binding at the predicted MIST1 binding site. The positions of the amplicon regions with respect to each gene are indicated *below the graphs*.

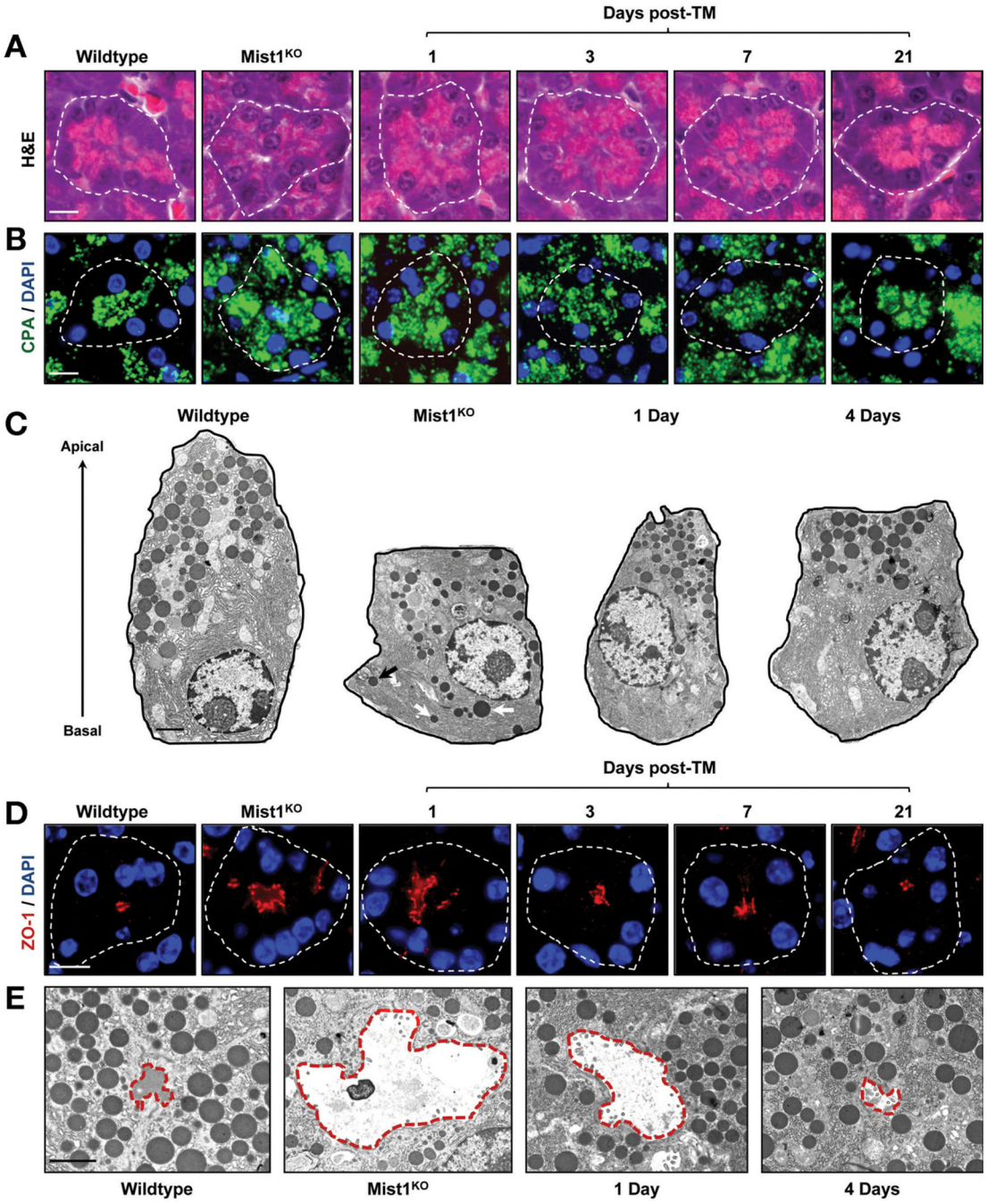

Figure 5.

Induced MIST1^{myc} rescues the *Mist1^{KO}* phenotype in adult acinar cells. (*A* and *B*) H&E and carboxypeptidase (CPA) immunofluorescence reveals the organization of zymogen granules within individual acini units of *WT, Mist1^{KO}*, and *Mist1^{KO}/LSL-Mist1^{myc}* pancreata 1, 3, 7, and 21 days after TM. (*C*) Transmission electron microscopy views of individual acinar cells showing the mislocalized zymogen granules (*arrows*) in *Mist1^{KO}* samples. (*D* and *E*) Analysis of lumen size in *WT, Mist1^{KO}*, and *Mist1^{KO}/LSL-Mist1^{myc}* acini by zonula occludens 1 (ZO-1) immunofluorescence and transmission electron microscopy. *White outlines*, individual acini; *red outlines*, individual lumens. DAPI, 4′,6-diamidino-2-phenylindole. *Scale bars*: (*A, B*, and *D*) 10 μm; (*C* and *E*) 2 μm.

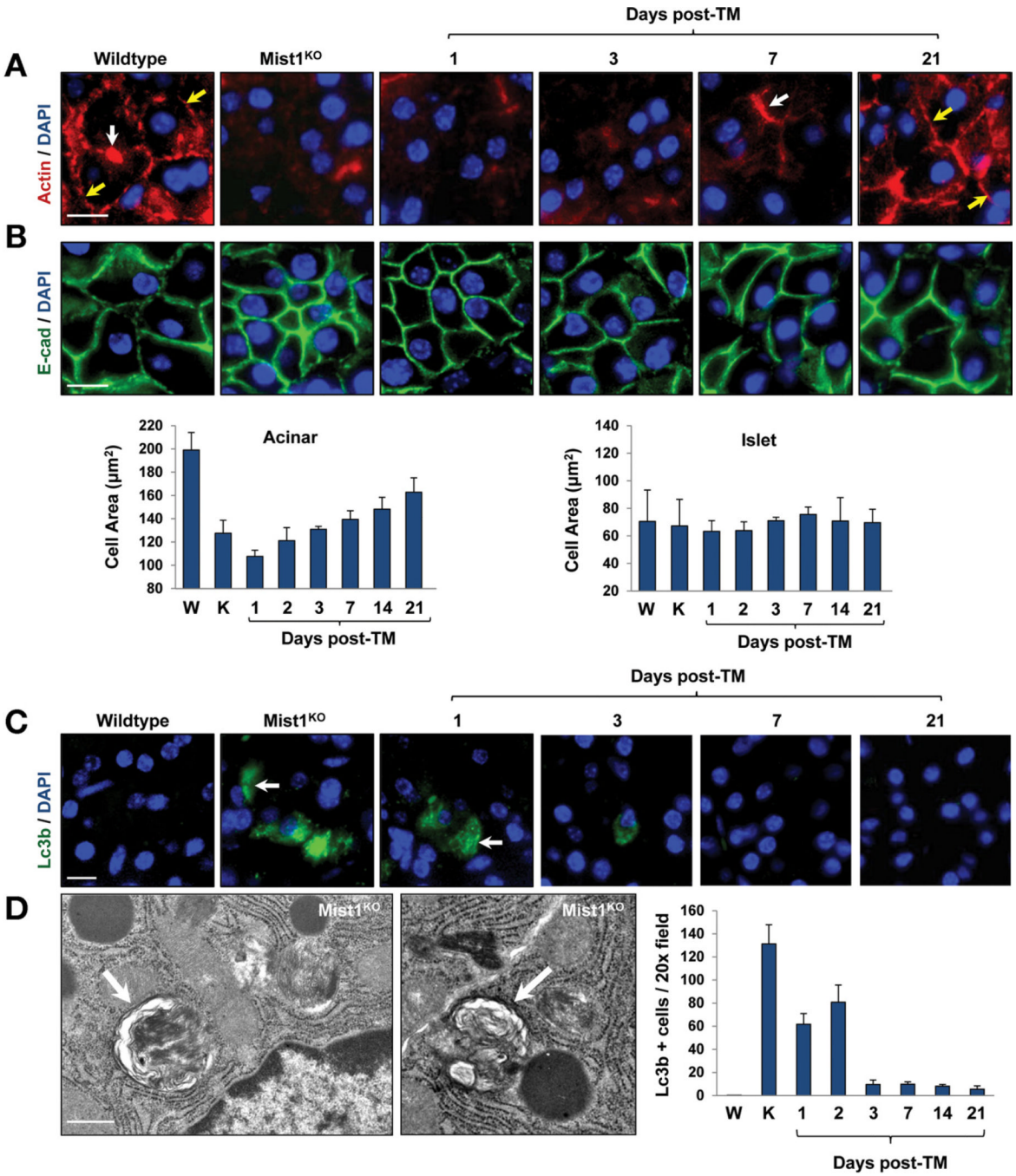

Figure 6.

Induced MIST1^{myc} rescues the actin cytoskeleton and cell size defects of *Mist1^{KO}* acinar cells. (*A*) Anti–β-actin immunofluorescence showing restoration of the terminal (*white arrows*) and cortical (*yellow arrows*) actin webs after TM-induced MIST1^{myc} expression. (*B*) E-cadherin immunofluorescence and quantification of acinar and islet cell areas over the TM time course. (*C* and *D*) LC3B immunofluorescence and TEM reveal that *Mist1^{KO}* acinar cells show high levels of autophagic vacuoles, whereas induced MIST1^{myc} expression reduces their presence to *WT* levels. (*C*) LC3B-positive cells (*arrows*); (*D*) individual autophagic vesicles (*arrows*). *Scale bars*: (*A, B*, and *C*) 10 µm; (*D*) 0.5 µm. DAPI, 4′,6-diamidino-2-phenylindole; E-cad, E-cadherin.

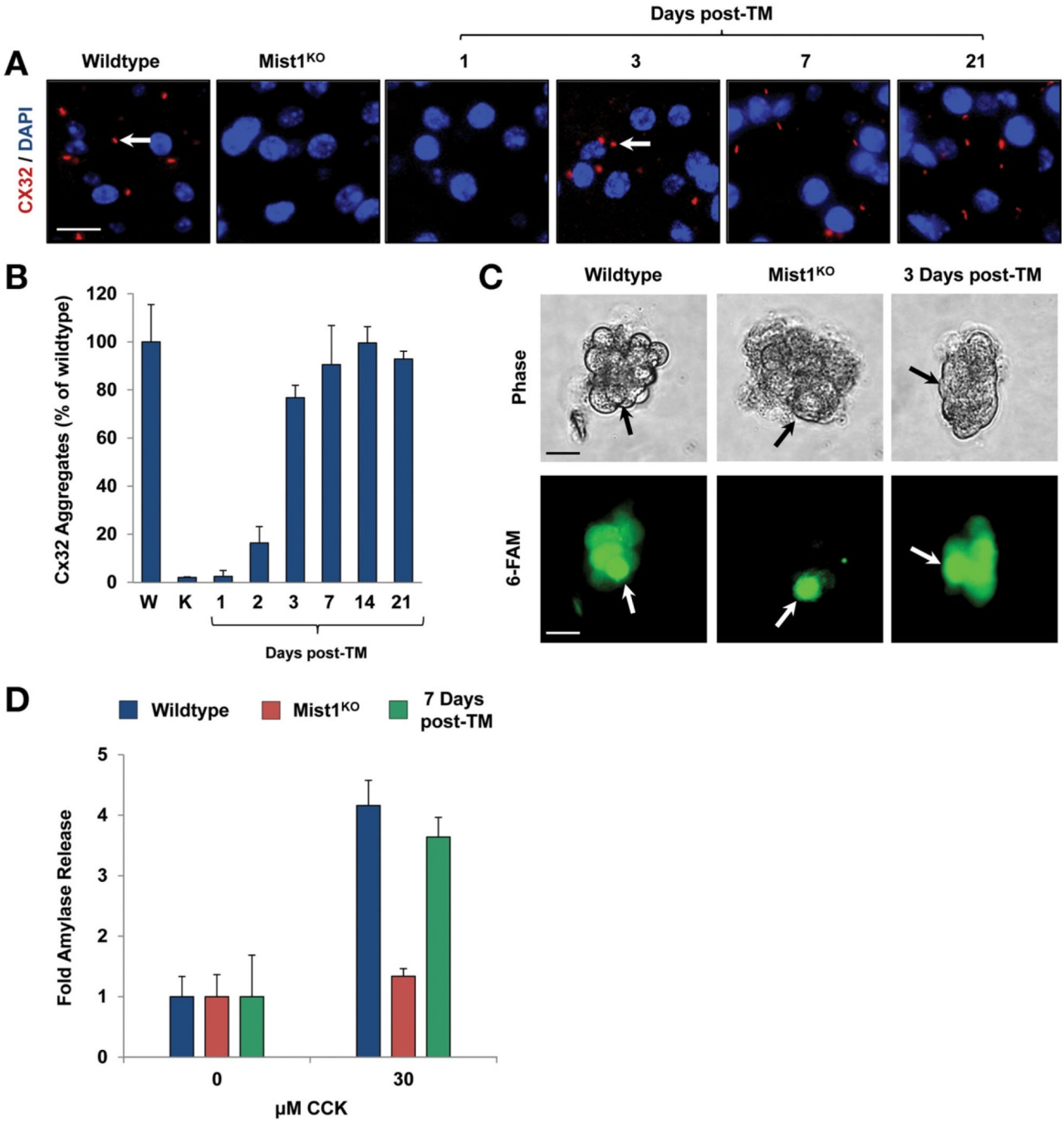

Figure 7.

Cx32-containing gap junctions, intercellular communication, and regulated exocytosis are rescued by MIST1^{myc} expression. (*A* and *B*) Cx32-containing gap junctions are produced upon *Mist1^{myc}* expression. *Arrows* show gap junction complexes. (*C*) Single-cell injections of 6-carboxyfluorescein (6-FAM) into isolated acini reveal that intercellular transfer of 6-FAM into neighboring acinar cells occurs after MIST1^{myc} induction. *Arrows* show the injected cell. (*D*) Quantification of amylase secretion from *WT, Mist1^{KO}*, and *Mist1^{KO}/LSL-Mist1^{myc}* acini after cholecystokinin (CCK) stimulation. The defect in secretion observed with *Mist1^{KO}* acinar cells is reversed completely by induced *LSL-Mist1^{myc}* expression. *Scale bars*: (*A*) 10 μm; (*C*) 20 μm. DAPI, 4′,6-diamidino-2-phenylindole.